Available online at www.sciencedirect.com
SCIENCE DIRECT®
Journal of Chromatography A, 1063 (2005) 79–88
JOURNAL OF CHROMATOGRAPHY A
www.elsevier.com/locate/chroma

Limits of multi-linear gradient optimisation in reversed-phase liquid chromatography

V. Concha-Herrera, G. Vivó-Truyols, J.R. Torres-Lapasió*, M.C. García-Alvarez-Coque

Departamento de Química Analítica, Facultad de Química, Universitat de València, c/Dr. Moliner 50, 46100 Burjassot, Spain

Received 21 July 2004; received in revised form 8 October 2004; accepted 1 December 2004

Abstract

The concept of limiting peak purity was applied to quantify the degree of completion of the separation capability of a chromatographic system using multi-linear gradients. The objective was to check whether the complexity of a gradient program deserves be increased to enhance resolution by inserting more linear segments, or on the contrary, no significant improvements can be expected under more complex gradients. A set of 19 isoindole derivatives of primary amino acids was selected to test the performance of isocratic, single linear and multi-linear gradients. Accurate simulated chromatograms were obtained via numerical integration of the general equation of gradient elution, using pre-established start and end conditions of the gradient program. The overall peak purity was selected as objective function. Good—although not baseline—resolution was achieved with an optimal trilinear gradient. Excellent agreement between experimental and predicted optimal chromatograms was found. With the proposed approach, a degree of completion of the separation capability of the chromatographic system of 21.2, 49.7, 81.5 and 88.5% was accomplished with optimal gradients with one, two, three and four segments, respectively. More complex gradients did not enhance the latter figure significantly. Also, multi-linear gradients gave rise to more benefits than complementary gradients.

Keywords: Gradient elution; Multi-linear gradients; Peak purity; Limiting resolution

1. Introduction

Nowadays, optimisation methods have exploited most possibilities of isocratic elution and a variety of efficient approaches are available [1–4]. This picture contrasts with the situation in gradient elution, which still requires major improvements to reach all its potential. Currently, linear gradients have displaced curved gradient profiles, since they are more easily reproduced in different instruments, and consequently, methods are easier to be transferred with accuracy [5]. However, a single linear step is often unable to resolve the analysed mixture and multi-segmented gradients are required.

In practice, chromatographs generate gradients by performing consecutive small isocratic steps, usually at increasing modifier concentration. An accurate approximation of a target sloped gradient requires a large number of these steps. However, gradients can also be approximated to a few large isocratic steps with a prefixed increment in solvent concentration (i.e. stepwise or multi-isocratic gradients) [6–10]. Recently, Nikitas et al. [10] derived new equations to predict gradient retention times in multi-isocratic gradient programs, with a stepwise variation pattern where the modifier concentration could be increased, or eventually, decreased, the former possibility being more interesting in practice.

Multi-linear approaches are good alternatives to multi-isocratic gradients. In this case, more than one segment of different slope is defined, where the modifier concentration is linearly increased. In order to speed up the elution, the gradient slopes should be always positive, but occasionally, one or more isocratic steps can be inserted, or the slope be decreased with respect to previous segments to get optimal separation for some solute bands. Software based on

* Corresponding author. Tel.: +34 963543003; fax: +34 963544436.
E-mail address: jrtorres@uv.es (J.R. Torres-Lapasió).

0021-9673/$ – see front matter © 2004 Published by Elsevier B.V.
doi:10.1016/j.chroma.2004.12.001

these ideas is commercially available (e.g. Osiris [11], Drylab [12]).

The most simple computer approach for multi-linear gradients consists of the insertion of nodes altering an optimal single-step linear gradient, assisted by the observation of simulated chromatograms [11–13]. Each node is dragged and dropped at will in a trial-and-error fashion. This strategy is especially suited when there are a few well-resolved peaks at the end of the chromatogram, where there is sufficient resolution to be the exact position of the node non-critical. The experience of the chromatographer is thus usually enough to find a satisfactory gradient. In the limit, this approach can be particularised to each solute cluster in the eluted mixture [14,15].

Similar to isocratic elution, grid searches have been developed to find out systematically the position of one, two or more nodes in multi-linear sloped gradients. However, the computation time for these approaches increases exponentially with the number of nodes, and the developers do not extend usually the application to more than two or three nodes [5,16–18].

In previous work [1,2], we proposed an optimisation methodology for isocratic elution where the product of peak purities (p) was maximised to obtain optimal separation conditions. This assessment has some intrinsic advantages related to the unambiguous association of one measurement to each solute, and its straightforward meaning (p-values range between 1 and 0 for null and full interference, respectively). We apply here the concept of peak purity to check whether the complexity of the gradient program deserves be increased by adding more linear segments to fully exploit all the capabilities of the solvent system. The proposed algorithm scans the possibilities of multi-linear gradients with pre-established start and end conditions of the gradient program. The method was applied to optimise the separation of the 19 primary proteic amino acids, previously derivatised with *o*-phthalaldehyde (OPA) and *N*-acetylcysteine (NAC) to form isoindoles, which were eluted with acetonitrile–water mobile phases at pH 6.5.

2. Theory

2.1. Simulation of chromatograms

The accuracy of the predicted retention times is a key point that influences the reliability of the optimisation study. Thus, achievement of good models able to describe the retention of the compounds of interest as a function of the factors(s) being varied during the gradient program is mandatory. Traditionally, gradient elution programs are optimised by changing the gradient slope and the initial mobile-phase composition, although other properties, such as temperature and pH, have been considered [11,12]. In this work, the subjacent experimental factor was the acetonitrile content in the organic mobile phase, and therefore, the studied gradients were restricted to this factor.

Any interpretive optimisation procedure relies on the fitting of experimental data to a retention model. This implies the development of an experimental design, that can be performed either under isocratic (i.e. measuring the retention of each compound at different mobile-phase compositions), or gradient (i.e. measuring the retention of each compound under different gradient programs) elution modes. Although gradient experimental designs may require less effort, the benefits are only full when all standards can be injected simultaneously, being the identity of each resulting peak known without ambiguity through peak tracking. If peak tracking is not conclusive or an adequate detector is not available, either the individual injection of each compound or the injection of reduced subsets of resolved compounds at each experimental condition are required for avoiding misidentification. This fact, together with the elimination of re-equilibration steps between consecutive injections can make a cleverly designed isocratic set of experiments fully competitive.

In addition to these considerations, isocratic designs are significantly more informative than gradient ones [19,20]. In this work, we selected isocratic elution for retention modelling to measure the maximal separation capability of the chromatographic system by applying the limiting purity concept (Section 4.4). Isocratic elution also allowed describing the retention behaviour with the highest accuracy level.

The retention was modelled using the most widely applied equations in reversed-phase liquid chromatography, the most appropriate for each solute being selected on an ANOVA basis:

$$\log k = c_0 + c_1\varphi \quad (1)$$

$$\log k = c_0 + c_1\varphi + c_2\varphi^2 \quad (2)$$

where k is the retention factor, φ the volume fraction of organic solvent (in this case, acetonitrile), and c_0, c_1 and c_2 the fitted parameters.

However, realistic simulations of chromatograms require the prediction of peak profiles. For this purpose, a modified-Gaussian model where the standard deviation depends linearly on the distance to the peak apex was selected [21]. This model includes parameters that can be related to the peak height (or area), efficiency (N), asymmetry (measured as B/A, B and A being the left and right halfwidths) and the retention time. The values of N and B/A were measured at 10% peak height for each solute at each isocratic condition of the experimental design. Efficiency was calculated according to Foley and Dorsey [22]. Linear or parabolic models were fitted to predict N and B/A as a function of mobile-phase composition [20]. Peak areas were normalised to the unity throughout this work, except in the comparison with experimental chromatograms.

The prediction of N and B/A is less accurate than the prediction of retention. One should note, however, that the factor with major impact in the resolution is the retention time.

Nevertheless, better predictions will be obtained for complex mixtures by considering variations in N and B/A with mobile-phase composition for each solute, with regard to those obtained either with the mean values of N and B/A within the experimental design, or just ignoring the peak shape influence.

Once built the models for retention, efficiency and asymmetry in isocratic mode, the next step is developing an algorithm able to take advantage of them to predict the separation under any gradient condition. For this purpose, the prediction of retention was performed through the resolution of the general equation for gradient elution:

$$t_0 = \int_0^{t_g - t_0} \frac{dt}{k(\varphi(t))} \tag{3}$$

where t_g is the retention time under gradient conditions, t_0 the retention of a non-retained compound, and $k(\varphi(t))$, the variation of the retention factor as a function of time. Note that the latter function is composed of two equations, namely, the variation of k versus φ (i.e. the retention model) and the variation of this factor with respect to time (i.e. the gradient program). Eq. (3) has an algebraic solution when Eq. (1) is used as retention model, and the gradient program is linear. Since this is not generally the case (as happens with multi-linear gradients, or when Eq. (2) is used), numerical integration is the most straightforward system to solve Eq. (3), although may mean long calculation times if used in optimisation.

Prediction of peak width under gradient conditions was carried out by applying the Jandera's approach [23]. This affirms that the band width of a given solute is equal to that observed if it were eluted isocratically, at the mobile phase affecting the solute when it reaches the column outlet during the gradient. The same basis was applied for predicting peak asymmetry [20].

2.2. Measurement of resolution

Optimisation is based on the improvement of a numerical value able to sum up the quality of the separation of the whole mixture in a given simulated chromatogram. This implies measuring and combining a set of elementary resolution values, each of them devoted to a particular solute. Several suitable criteria can be found in the literature for the evaluation of the resolution [24,25], whose advantages and drawbacks have been extensively discussed and are out of the scope of this work. We use here the peak purity concept, which is defined as the area fraction of a given solute i that is not overlapped by the chromatogram formed by the sum of its interferents [2]:

$$p_i = 1 - \frac{o_i'}{o_i} \tag{4}$$

where o_i' is the overlapped area under the peak of solute i, and o_i is its total area. Peak purity values for each solute and mobile phase were computed from chromatograms simulated according to Section 2.1.

The p_i elementary values associated to n solutes eluted under a given gradient program were combined in an overall peak purity value, through the dot product of the individual peak purities extended to all solutes. This was the objective function being maximised:

$$P = \prod_{i=1}^{n} p_i \tag{5}$$

The process of calculation of overall purity is generally extended to a predefined set of experimental conditions (i.e. a set of isocratic experiments or a set of gradients), eventually obtaining a $\boldsymbol{P}$ vector or matrix (according to the number of factors being varied). The position of the element in $\boldsymbol{P}$ with a maximal value will denote the optimal separation conditions. Alternatively, the process can be applied to the elementary purity vector (or matrix) of a given solute (instead to the global purity vector/matrix). For each solute in the mixture, there will be a certain experimental condition that will give its best separation from all the others. Associated to this separation condition, there is a maximal elementary resolution value for that solute, which has been called the limiting peak purity [26]. If the solute can reach full separation, the limiting purity will be 1.0. When in the best conditions there is a certain overlap with other(s) solute(s), it will be <1.

Limiting purity is a useful concept to prospect the maximal separation capability of a chromatographic system in order to separate, either a given solute or a set of solutes from the others. Based on this assessment, a special optimisation that takes maximal advantage of the system capability was proposed, namely, the complementary mobile-phases optimisation [2,26]. This methodology consists of finding a number of optimal chromatographic conditions (e.g. two or three mobile-phase compositions or/and columns), selected in such a way that each one is devoted to get an optimal separation of a given subset of compounds. When the results of all conditions are considered globally, all compounds should be maximally resolved and the overall purity should tend to the overall limiting purity.

2.3. Gradient optimisation

The aim of this work was developing a measurement that allows establishing the theoretically maximal resolution capability that can be expected using multi-linear gradient elution, in order to decide if the introduction of new nodes will produce significant benefits on resolution. The efficiency of the optimisation algorithm was out of our concern: a more sophisticated algorithm would lead to the same results, although in less time. For this reason, we selected a grid search as optimisation algorithm, which although being slow, was anyway enough for our purposes.

The dwell time, t_D (the time delay between gradient formation and column inlet), was considered as an initial iso-

cratic step always present in any scanned gradient program. This means that actual gradient profiles should be obtained by adding t_D to the programmed time values. However, for simplicity, figures showing 3D views and contour maps of resolution surfaces in this work do not include in the axis the dwell time, although it was obviously considered in the calculations.

2.3.1. Simple linear gradient optimisation

The optimisation of gradients was first tackled by performing a grid search of gradient slopes and initial solvent concentrations (i.e. the factors defining each gradient program), assessing the performance of all possible combinations of gradient descriptors. This yielded a resolution curve (one-factor optimisation: gradient slope), or surface (two-factor optimisation: gradient slope and initial solvent concentration). The detail level in the resolution surface was governed by the coarseness (t_c and φ_c), which is the increment in the considered experimental factor.

2.3.2. Multi-linear gradient optimisation

This work evaluates the possibilities of gradient separation using two or more consecutive linear gradients. For this purpose, the most conventional approach of defining a single linear gradient by fixing initial (φ_0) and final (φ_f) solvent contents, and setting a transition time (t_f), was chosen. The complexity of the multi-linear gradient program is determined by the number of nodes (n). The most straightforward gradient program is defined for $n = 0$, which means a program without nodes, varying linearly from φ_0 to φ_f in t_f. The insertion of one node at (t_1, φ_1), gives rise to a two-segment gradient (i.e. a bilinear gradient). Any gradient program selected for $n = 1$ increases linearly from φ_0 to φ_1 in t_1, and then reaches linearly φ_f in $t_f - t_1$. This intermediate condition is always selected accomplishing that $\varphi_0 < \varphi_1 < \varphi_f$ and $t_0 < t_1 < t_f$. All possibilities in the position of this first node were prospected by considering the selected coarseness in φ and t: $\varphi_1 = \varphi_0$, $\varphi_0 + \varphi_c$, $\varphi_0 + 2\varphi_c$, ..., φ_f and $t_1 = t_0$, $t_0 + t_c$, $t_0 + 2t_c$, ..., t_f. The algorithms for gradient elution explained in Sections 2.1 and 2.2 were applied, yielding thus vectors of elementary and global peak purities for each tested gradient program.

Gradient optimisation can be sophisticated and adapted to the particularities of the sample by inserting a larger number of nodes. This will increase also the possibilities of success in the separation of the mixture, but with the inconvenience of requiring larger computation times. For $n = 2$, a pair of intermediate conditions should be defined: (t_1, φ_1) and (t_2, φ_2). In this case, the gradient program increases linearly the concentration of modifier from φ_0 to φ_1 in t_1, then to φ_2 in $t_2 - t_1$, and finally, to φ_f in $t_f - t_2$. Both nodes were selected accomplishing $\varphi_0 < \varphi_1 < \varphi_2 < \varphi_f$ and $t_0 < t_1 < t_2 < t_f$. Note that these conditions assure that the gradient always yields an increase in elution strength. As in the case of $n = 1$, all combinations of two nodes were scanned by considering the coarseness in t and φ. From a theoretical standpoint, there is no limit in the number of nodes considered in the optimisation, although when $n > 3$ the required computation time begins to constitute a limit that constrains the practical application of the algorithm.

3. Experimental

3.1. Reagents

The reagent mixture contained *o*-phthalaldehyde, *N*-acetylcysteine (Fluka, Buchs, Switzerland), and a buffer prepared with boric acid (Probus, Badalona, Spain). The 19 studied *L*-amino acids (Table 1) were obtained from diverse manufacturers. Other chemicals needed were ethanol (Merck, Darmstadt, Germany), sodium hydroxide (AnalaR, Poole, UK), and hydrochloric acid (Panreac, Barcelona, Spain). Mobile phases were prepared with acetonitrile (HPLC grade, Scharlab, Barcelona). Mobile-phase pH was buffered using trisodium citrate dihydrate and a convenient amount of hydrochloric acid (Merck). All reagents were of analytical grade.

The mobile phases and the solutions of the OPA-NAC derivatives were filtered through 0.45 μm membranes (Micron Separations, Westboro, MA). Nanopure water was used throughout (Barnstead, Sybron, Boston, MA).

3.2. Apparatus and software

The chromatograph (Agilent, Model HP 1100, Waldbronn, Germany) was equipped with a quaternary pump, a column oven, an automatic sampler, and a diode-array detector. The separation was carried out with a 250 mm × 4.6 mm i.d. Inertsil ODS3 column with 5 μm particle size (Análisis Vínicos, Tomelloso, Spain), connected to a 30 mm × 4 mm

Table 1
Prediction errors for the 19 OPA-NAC amino acid derivatives

Code	Amino acid	R.E.[a]	R^2_{adj} [b]
1	Aspartic acid	0.01	1.0000
2	Glutamic acid	0.04	1.0000
3	Asparagine	0.24	1.0000
4	Serine	0.26	0.9999
5	Glutamine	0.40	1.0000
6	Histidine	0.22	1.0000
7	Threonine	0.22	1.0000
8	Glycine	0.28	1.0000
9	Arginine	0.26	0.9999
10	Alanine	0.39	0.9999
11	Tyrosine	0.56	0.9999
12	Cysteine	2.36	0.9985
13	Valine	0.44	0.9999
14	Methionine	0.30	0.9999
15	Isoleucine	0.32	0.9999
16	Lysine	0.13	1.0000
17	Tryptophan	0.13	1.0000
18	Phenylalanine	0.06	1.0000
19	Leucine	0.03	1.0000

[a] The percentage of relative error (R.E.) was calculated according to [27].
[b] Corrected determination coefficient.

i.d. Kromasil C18 guard column with 5 μm particle size (Scharlab). The column temperature was fixed throughout at a nominal value of 25 °C, and the flow-rate was kept constant at 1 ml/min. Detection of amino acid derivatives was performed at 335 nm.

The dead time (2.1 min) was measured from the first deviation of the baseline, whereas the dwell time (1.79 min) was obtained by monitoring at 280 nm a blank gradient where acetone was increased from 0 to 1% in 20 min [28].

Home built-in routines, written in MATLAB 6.5 (The Mathworks, Natick, MA), were developed for data treatment.

3.3. Derivatisation and chromatographic procedures

The OPA-NAC reagent, prepared weekly by mixing in this order an ethanolic OPA solution, an aqueous boric acid/borate buffer, and NAC solution, was stored at 4 °C protected from light by covering the solution with aluminium foil. The final concentrations of the reagents were 2.5×10^{-4} M OPA, 4.0×10^{-4} M NAC, and 0.1 M boric acid/borate buffer. Stock amino acid solutions (1.5×10^{-3} M) were diluted with water up to 6.0×10^{-6} M before injection into the chromatograph, except for cysteine (1.8×10^{-5} M), which showed lower absorptivity.

The derivatives were formed by mixing an aliquot of each amino acid solution with 3 ml of the OPA-NAC reagent, and diluting to 10 ml with water. After 10 min, 20 μl of the derivatives was injected into the chromatograph, and eluted under isocratic or gradient elution with acetonitrile–water mixtures, where pH was fixed at 6.5 with 5.0×10^{-3} M citric acid/citrate buffer. Duplicate injections were made.

4. Results and discussion

4.1. Experimental design and retention modelling

A separation problem, containing the 19 proteic amino acids was selected to test the proposed method. The OPA-NAC derivatives were eluted with isocratic mixtures of acetonitrile–water at pH 6.5. The acetonitrile working range was 5–27.5%. However, due to the large differences in polarity among amino acid derivatives, only some mobile phases were suitable to elute each solute in appropriate analysis times. Depending on the solute, data corresponding to 4–6 mobile-phase compositions were available to build the different models describing the isocratic retention, efficiency and asymmetry factor.

Table 1 lists for each derivative the errors obtained in the prediction of retention, which were extremely low for all amino acids. Only cysteine showed a larger relative error, although anyway very low. Nevertheless, the comparison of the experimental optimal chromatograms with the predicted ones (Section 4.3) constitutes the most demanding validation procedure of any prediction method. In addition, it should be noted that the validity of the selected retention models has been exhaustively tested for decades. The limits of the considered search space for all gradients involved in the optimisation studies shown below were from $t_0 = 0$ to $t_f = 80$ min, and from $\varphi_0 = 5$ to $\varphi_f = 27.5\%$ acetonitrile, which equals the range covered by the isocratic experimental design. We did not consider convenient to predict gradients whose initial concentration is below 5% acetonitrile, which would mean an extrapolation. On the other hand, retention times for >27.5% acetonitrile were too low for most amino acid derivatives, which appeared overlapped, and for these concentrations modelling was considered useless.

4.2. Simple linear gradient optimisation

Fig. 1a depicts the resolution map for the two-factor (φ_0 and t_G) gradient optimisation. Slices of this plot, parallel to the t_G axis (i.e. at fixed φ_0) would yield one-factor (t_G) window diagrams of products of peak purities. The best results were achieved by starting the gradient program at 5.0% acetonitrile, with 75.3 min as gradient time. The coarseness values for t_c and φ_c were 1.33 min and 0.5% acetonitrile, respectively, which corresponded to a 54×6 simulation design. As can be seen, the optimum found yielded poor resolution ($P \approx 0.20$, Table 2), which is evidenced by the corresponding predicted chromatogram (Fig. 2a). A severe overlap is observed between compounds 12/13 and 16/18/19, and to a lesser extent, for compounds 7/8. A single-step gradient optimisation was thus not satisfactory for this mixture.

4.3. Multi-linear gradient optimisation

The resolution surface and the optimal chromatogram obtained for a bilinear gradient optimisation (i.e. multi-linear gradient with one node) are shown in Figs. 1b and 2b, respectively. The selected coarseness for t_c was 4 min, and for φ_c, 1.12% acetonitrile, which gave rise to a 21×21 simulation design. In this case, since the initial and final (t, φ) values were fixed, only two factors were optimised: those defining the coordinates of the unique node (t_1, φ_1). Therefore, this optimisation looks like a conventional isocratic two-factor optimisation. The optimal gradient achieved with the proposed algorithm included an initial ramp going from 5 to 17.4% acetonitrile in 56 min, reaching then 27.5% acetonitrile in additional 24 min (see dashed lines in Fig. 2b). It should be observed that the node is located in the neighbourhood of the diagonal elements of the resolution surface, which means that the optimal bilinear gradient program is close to the linear one (which goes directly from φ_0 to φ_f in t_f min). This can be confirmed if one inspects the gradient plot in Fig. 2b, in which the slopes of both segments of the gradient program are rather similar (0.28% min^{-1} for the unique segment of the linear gradient, and 0.22 and 0.42 min^{-1} for the two segments of the bilinear gradients).

All gradient programs located in the diagonal region in Fig. 1b, which apparently seem different according to the

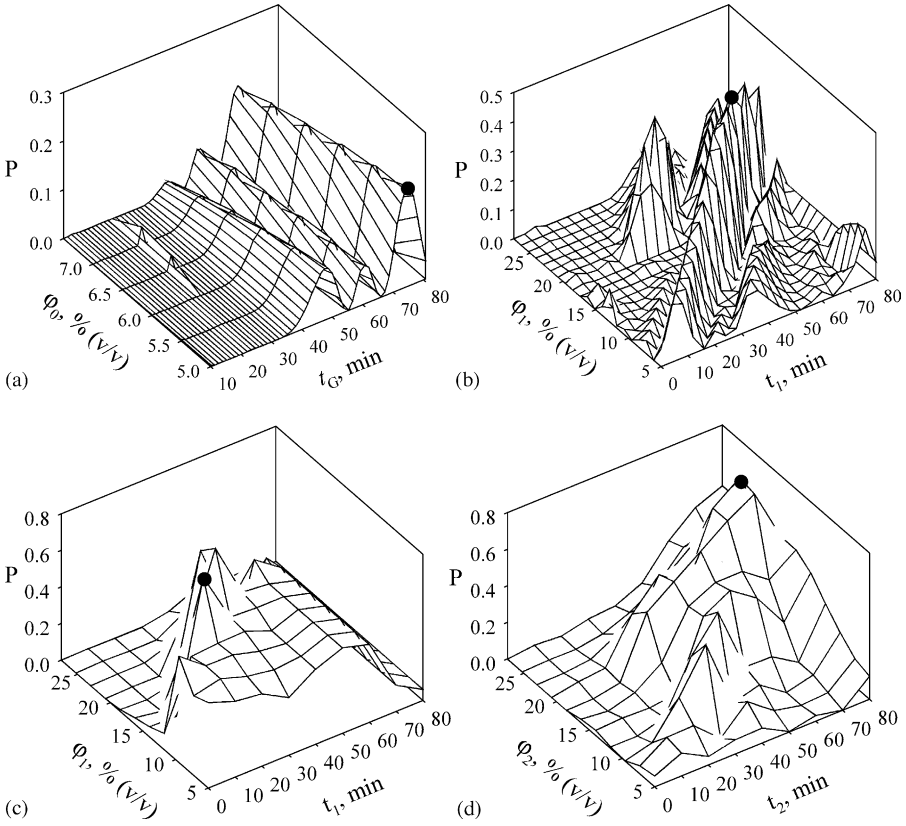

Fig. 1. Overall purity surfaces at varying gradient time (t_G) and initial concentration of acetonitrile (φ_0) for the separation of the 19 OPA-NAC amino acid derivatives by applying: (a) linear, (b) bilinear, and (c and d) trilinear optimisations. The black dot indicates the optimal condition.

Table 2
Optimal (p_{opt}) and limiting (p_L) purities for the gradient and isocratic optimisations in the separation of the 19 OPA-NAC amino acid derivatives

Compounds[a]	Linear		Bilinear		Trilinear		Tetralinear		Isocratic
	p_{opt}	p_L	p_{opt}	p_L	p_{opt}	p_L	p_{opt}	p_L	p_L
1	1.000	1.000	1.000	1.000	1.000	1.000	1.000	1.000	1.000
2	1.000	1.000	1.000	1.000	1.000	1.000	1.000	1.000	1.000
3	1.000	1.000	1.000	1.000	1.000	1.000	1.000	1.000	1.000
4	1.000	1.000	1.000	1.000	1.000	1.000	1.000	1.000	1.000
5	1.000	1.000	1.000	1.000	1.000	1.000	1.000	1.000	1.000
6	1.000	1.000	1.000	1.000	1.000	1.000	1.000	1.000	1.000
7	0.945	0.953	0.956	0.972	0.936	0.977	0.939	0.979	0.979
8	0.945	0.952	0.956	0.972	0.934	0.977	0.938	0.979	0.979
9	1.000	1.000	1.000	1.000	0.998	1.000	1.000	1.000	1.000
10	1.000	1.000	1.000	1.000	1.000	1.000	1.000	1.000	1.000
11	1.000	1.000	1.000	1.000	1.000	1.000	1.000	1.000	1.000
12	0.805	1.000	1.000	1.000	0.969	1.000	0.999	1.000	1.000
13	0.805	1.000	1.000	1.000	0.970	1.000	0.999	1.000	1.000
14	1.000	1.000	1.000	1.000	1.000	1.000	1.000	1.000	1.000
15	1.000	1.000	1.000	1.000	1.000	1.000	1.000	1.000	1.000
16	0.767	1.000	0.945	1.000	1.000	1.000	1.000	1.000	1.000
17	1.000	1.000	0.994	1.000	1.000	1.000	1.000	1.000	1.000
18	0.571	0.875	0.722	0.939	0.976	0.997	0.982	0.999	1.000
19	0.802	0.871	0.770	0.917	0.976	0.997	0.982	0.999	1.000
Overall	0.203	0.691	0.477	0.815	0.782	0.949	0.849	0.957	0.959
Completion (%)	21.2	72.1	49.7	85.0	81.5	99.0	88.5	99.8	–

[a] See Table 1 for compound identities.

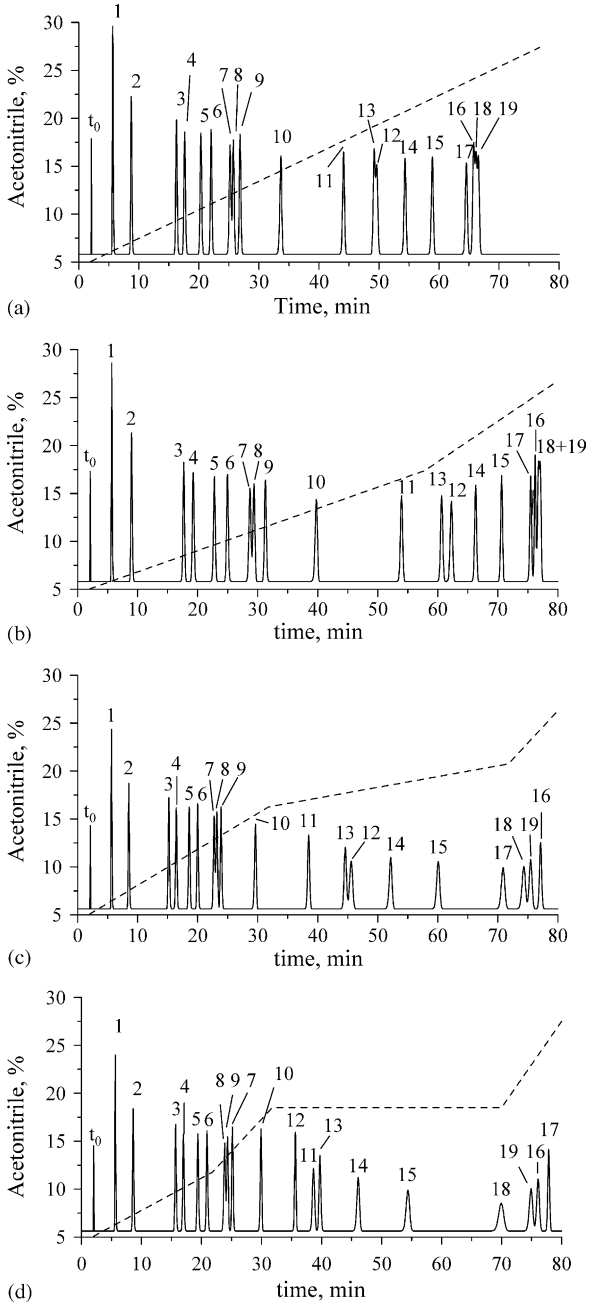

Fig. 2. Optimal chromatograms attending to the overall purity for a mixture of 19 OPA-NAC amino acid derivatives under different chromatographic situations by applying: (a) linear, (b) bilinear, and (c and d) trilinear gradients. The dashed line depicts the gradient program. See Table 1 for compound identities.

coordinates of the node (t_1, φ_1), indeed represent the same underlying increment in solvent, and as a consequence, yield similar resolution. Gradients represented by nodes close to the diagonal (with an almost constant variation in solvent composition as a function of time) can be also expected to yield similar resolution, but in addition, there are other apparently different gradients representing similar solvent increments. These gradients tend to yield linear resolution features. The main secondary structure belongs to one of these parallel structures, and presents the maximum at $t_1 = 36$ min, $\varphi_1 = 20.75\%$ acetonitrile.

The optimal overall purity using bilinear optimisation was $P \approx 0.48$, which is significantly larger than the value obtained for single linear gradients. As can be seen, the resolution of some compounds was still not satisfactory (see, e.g. the group of peaks 16/18/19). The multi-linear gradient approach offers the possibility of increasing the number of nodes as desired, that is, each segment can be focused on the separation of a specific solute cluster. If the optimal resolution achieved using n nodes is not satisfactory, the chromatographer can incidentally prospect an optimum for $n+1$ nodes through computer simulation, without the need of additional experimental work. This procedure can be repeated till reaching the chromatographer's satisfaction and/or the separation limits of the chromatographic system. The convenience of including more nodes and the way of assessing the real requirement of these new nodes will be discussed in Section 4.4.

In the case of trilinear gradients (i.e. three segments and two nodes), the resolution surface require a five-dimensional plot (four factors: t_1, t_2, φ_1 and φ_2, plus the resolution assessment itself), which cannot be properly drawn. Simplified diagrams can be obtained instead, by depicting the optimal resolution surface for each node. Fig. 1c and d show these resolution surfaces, and Fig. 2c the optimal chromatogram. For the first node (Fig. 1c), each point of the surface represents the maximal resolution achieved when that node is at the plotted position and the second one is at the optimal position. A similar idea, but fixing the second node, yields the second plot (Fig. 1d). These resolution diagrams, although being a simplification of the reality (which is highly more complex), give at least a graphical idea of the robustness of the optimum found. In the examined example, the optimal position of the first node is more critical than that of the second node. The reason is that this node is chosen in a later stage of the gradient and will not affect the compounds preceding the first node. Moreover, once fixed the first node, the second one should be chosen from a more reduced factor space. Another consideration to be taken into account is that the gradients along the main diagonal are more robust, due to geometrical reasons, since they represent closely similar underlying solvent increments.

Plots in Fig. 1c and d were generated by sampling less comprehensively the factor space, in comparison with the plots shown in Fig. 1a and b. The reason was the exponential increment in calculation time at increasing number of nodes. This was partially avoided by modifying the coarseness: t_c and φ_c were set to 10 min and 2.25% acetonitrile, respectively (compare with 4 min and 1.12% acetonitrile for the bilinear gradient optimisation), which corresponds to a 9×11 simulation design.

The optimum found in the new conditions increased significantly the resolution achieved with the bilinear optimisation, reaching an acceptable value ($P = 0.78$ instead of 0.48). This can be confirmed if one inspects the optimal chro-

matogram (Fig. 2c): the resolution of peaks 16/18/19 was improved till almost baseline. Compounds 12 and 13 were also satisfactorily resolved, and only a partial overlap remained between compounds 7 and 8. A small increase in the resolution was obtained by introducing a third node (Fig. 2d) ($P = 0.85$). The tetralinear gradient profile was similar to the trilinear, with a new node at 20 min inserting a horizontal segment.

Critical peaks correlate well with the position of the nodes. Thus, the node in the bilinear optimisation (Fig. 2b) is related mainly with the separation of peak pair 12/13, which obliges to increase slowly the concentration of organic modifier before the node to avoid their coelution (compare with Fig. 2a). Once these peaks left the column, the concentration of solvent can be steeply increased to elute the remaining compounds in the prefixed maximal gradient time. For the trilinear optimisation, the first node was shifted to shorter times (30 min versus 56 min for the bilinear optimisation, compare Fig. 2b and c), which does not affect significantly the resolution of the first peaks. However, if the slope of the gradient were not changed beyond 30 min, it would be detrimental for the separation of peaks 12/13 and 16/18/19, which would appear less resolved. This explains the fact that the optimal slope beyond the first node be strongly reduced. The second node is located just before reaching the final subset 16/18/19, which is translated in a strong increment in the slope to be able to reach the final gradient conditions. The resolution of these three peaks is achieved thanks to the moderate elution strength during the first and second segments.

Fig. 3 depicts predicted (Fig. 3a, c and e) and experimental (Fig. 3b, d and f) chromatograms for different gradient programs. Chromatograms a and b correspond to the secondary optimum found with linear gradients (optimising both t_G and φ_0). Note that this chromatogram is faster than the optimal situation shown in Fig. 2a. The other depicted chromatograms correspond to the optimisation of trilinear gradients (Fig. 3c–f). Fig. 3e and f show the chromatograms for a trilinear gradient where the optimum was chosen with certain time restrictions. In all cases, the agreement between predicted and experimental chromatograms is excellent.

The bottleneck of the gradient optimisation is the numerical computation of Eq. (3), since a systematic scanning of all possible multi-linear gradients is carried out. In order to keep the calculation time in a reasonable figure, we took the decision of decreasing the grid thickness and the accuracy of numerical integration. The treatment based on these simplifications does not guarantee the true optimal separation be found. Nevertheless, the final simulation at the optimal conditions was performed at the highest possible accuracy level. In case of disagreement with the corresponding experimental chromatograms, the optimisation should be repeated at a higher accuracy, incidentally shrinking the factor space to a more restricted region. However, the agreement between experiments and predictions was good and the mentioned improvement was not required.

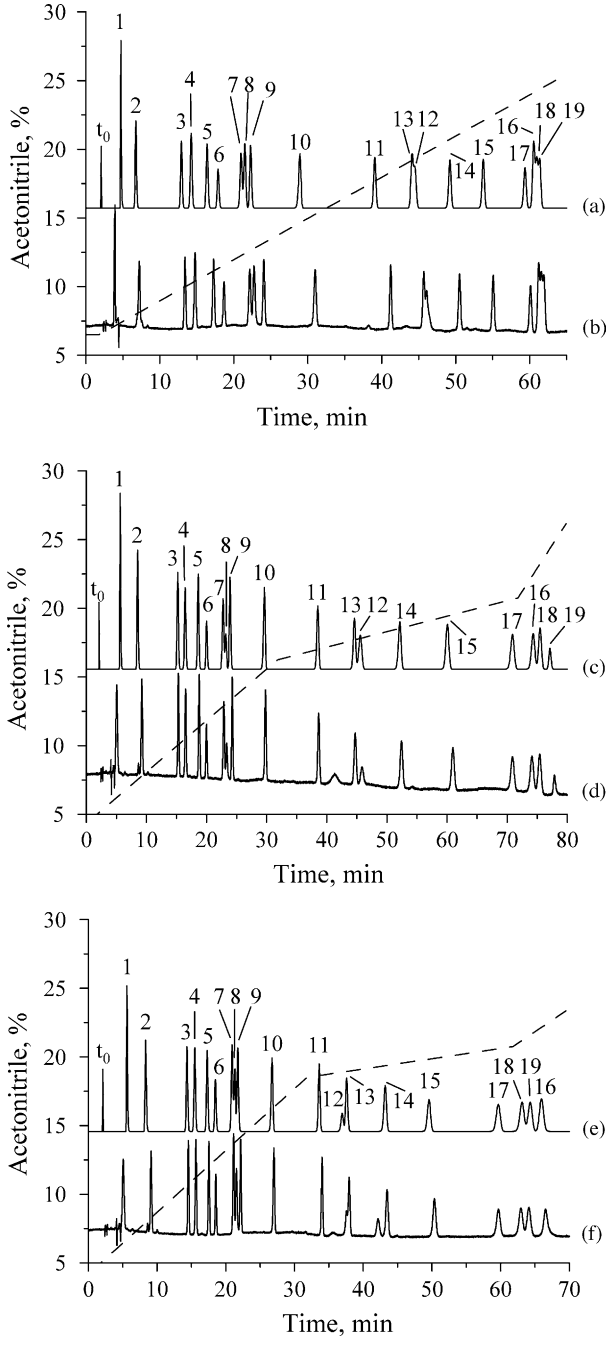

Fig. 3. Predicted (a, c, and e) and experimental (b, d, and f) chromatograms for several optimal gradient programs: (a) ($\varphi_0 = 5.0\%$, $t_G = 75.3$ min), (b) ($\varphi_0 = 5.0\%$, $\varphi_f = 27.5\%$, $t_f = 80$ min), ($\varphi_1 = 16.25\%$, $t_1 = 30$ min) and ($\varphi_2 = 20.75\%$, $t_2 = 70$ min), and (c) ($\varphi_0 = 5.0\%$, $\varphi_f = 27.5\%$, $t_f = 80$ min), ($\varphi_1 = 18.5\%$, $t_1 = 30$ min) and ($\varphi_2 = 20.75\%$, $t_2 = 60$ min). See Table 1 for compound identities. Experimental areas were used for updating simulations.

4.4. Limiting purities as tools for scanning multi-linear gradient complexity

The above results illustrated the advantage of introducing a more complex gradient program to accommodate the requirements of each peak cluster. Thus, the overall peak

purity increased from $P = 0.20$ to 0.48 to 0.78 to 0.85 for single, bilinear, trilinear and tetralinear gradients, respectively. The point is to anticipate how many nodes will improve significantly the resolution without the need of performing the corresponding full optimisation.

Limiting purities have demonstrated to be a useful tool to quantify the extent in which a given experimental condition has been able to exploit the resolution capability of the system [2]. Table 2 shows the elementary peak purities at the optimal composition, together with the limiting values, for four types of gradient separations: linear, bilinear, trilinear and tetralinear, together with the results of the isocratic separation, which is given as reference. The latter column constitutes the maximal capability of the system, since it expands the separation among peaks. In fact, the isocratic limiting purities indicate that the chromatographic system is able to separate all peaks up to the baseline, except threonine and glycine (compounds 7 and 8), which reach almost isolation. However, the isocratic elution of the amino acid derivatives under the theoretically optimal separation conditions implies absolutely unpractical analysis times. The interest of presenting isocratic limiting purities is that they indicate whether the system will be able to resolve the compounds under gradient elution: if the isocratic limiting values for two or more peaks are below a given threshold, no single linear or multi-linear gradient will be able to separate the mixture. Thus, isocratic limiting values are ideal figures that allow prospecting the maximal capabilities of the chromatographic system under both isocratic and gradient elution.

The meaning of limiting purities in gradient elution is similar to the isocratic limiting values: for each solute, they will indicate the minimal degree of interference that can be expected. Thus, as can be seen in Table 2, the optimal linear gradient is far below the system capability described by the isocratic values ($P_L = 0.203$ versus 0.959). The same holds for the limiting purity for this kind of gradient ($P_L = 0.691$), so the introduction of nodes can be expected to yield benefits. The same picture is observed for one and two nodes. The overall limiting purity is $P_L = 0.815$ and 0.949 for the bilinear and trilinear gradients, respectively. The latter value almost equals the isocratic limiting purity ($P_L = 0.949$ versus 0.959), therefore a third node (with $P_L = 0.957$) will not contribute appreciably to the enhancement of resolution.

A degree of completion of the separation capability of the chromatographic system of 21.2, 49.7, 81.5 and 88.5% was accomplished for optimal gradients with one, two, three and four segments, respectively. These figures are obtained by dividing the limiting purity in the selected separation by the isocratic limiting resolution (Table 2). More complex gradients will not enhance the separation significantly. On the other hand, the optimal overall purity becomes closer to the overall limiting value as the number of nodes increases. Changes in elution order in isocratic mode can appear or not in gradient mode. However, if no peak reversal happens in isocratic mode, no peak reversal will be observed in gradient mode, provided that the isocratic experiments cover appropriately the gradient scans.

Similar to isocratic elution, an approach has been reported where the solutes were optimally resolved by performing two runs at different temperature and gradient times (complementary linear gradients) [29]. The relative performance of complementary gradients versus multi-linear gradients can be also evidenced from the resolution values listed in Table 2. Under ideal conditions, two or more optimal complementary linear gradients would yield $P = 0.691$ (the larger the number of optimised complementary gradients, the closer to this figure). Note that one optimal bilinear gradient gives rise to an appreciable increase in the overall purity with respect to the single linear gradient, and that the optimal purity for the trilinear gradient is even larger than the theoretical largest resolution achieved with several complementary linear gradients, tending to the maximal separation capability of the system. Including a larger number of segments in the gradient optimisation, gives rise to more opportunities to adapt the system to the particularities of each solute cluster, getting thus the elementary resolutions closer to the limiting ones.

As indicated above, glycine and threonine coelute under any isocratic condition. This behaviour is replicated under any assayed gradient. Accordingly, the only possibility of enhancing the separation of this peak pair is a major change in the nature of the chromatographic system (e.g. column, solvent system, pH or temperature).

5. Conclusions

An efficient inspection of the resolution capability of a chromatographic system can be performed by applying the concept of limiting purity. In isocratic elution, the only way to achieve the full resolving capability, when the complexity of the mixture is high, is the use of complementary mobile phases. In gradient elution, however, the inclusion of nodes to particularise the requirement of each peak cluster becomes a competitive alternative to exploit the full capability of the system, making the resolution closer to the maximal values. From a practical point of view, the use of multi-linear gradients present more advantages than developing two or more complementary gradients.

The number of steps or segments showing particular gradient slopes can be increased at will, but the computation time increases exponentially. The same holds for the complementary gradients. The research presented in this work was developed in a PC provided with a 3 GHz Pentium IV processor. In such a computer, the calculation time for determining the best linear, bilinear, trilinear and tetralinear gradients was 1.6, 2.2, 13.6 min and 8.4 h, respectively, which should be enhanced. This will be the subject of future work.

The use of gross grids expedited the calculation time. However, it cannot be discarded that a close situation (not included in the studied grid) could enhance slightly the op-

timal gradient separation with n nodes. Note that the reference results correspond to isocratic elution, and are calculated with high accuracy. Consequently, if the optimisation were developed using a thicker grid, the trend of converging will happen at slightly higher purity values, but the threshold will not change.

Acknowledgements

This work was supported by Projects CTQ2004–02760/BQU (Ministerio de Educación y Ciencia of Spain) and Groups Grant 04/16 (Generalitat Valenciana). VCH, who is on leave from the University of Zacatecas (Mexico), thanks a Ph.D. fellowship from PROMEP (Mexican Government). GVT thanks the Generalitat Valenciana for an FPI grant. JRTL thanks the MCYT and the Generalitat Valenciana for a Ramon y Cajal position.

References

[1] J.R. Torres-Lapasió, M. Rosés, E. Bosch, M.C. García-Alvarez-Coque, J. Chromatogr. A 886 (2000) 31.
[2] G. Vivó-Truyols, J.R. Torres-Lapasió, M.C. Garcia-Alvarez-Coque, J. Chromatogr. A 876 (2000) 17.
[3] W.D. Beinert, V. Eckert, S. Galushko, V. Tanchuk, I. Shishkina, LaborPraxis 26 (2002) 16.
[4] T.H. Hoang, D. Cuerrier, S. McClintock, M. di Maso, J. Chromatogr. A 991 (2003) 281.
[5] T. Jupille, L. Snyder, I. Molnar, LCGC Europe 596 (2002) 2.
[6] W. Golkiewicz, Chromatographia 21 (1986) 259.
[7] R. Cela, M. Lores, Comput. Chem. 20 (1996) 175.
[8] R. Cela, J.A. Martínez, C. González-Barreiro, M. Lores, Chemom. Intel. Lab. Syst. 69 (2003) 137.
[9] M. Hutta, R. Góra, J. Chromatogr. A 1012 (2003) 67.
[10] P. Nikitas, A. Pappa-Louisi, K. Papachristos, J. Chromatogr. A 1033 (2004) 283.
[11] Osiris, Datalys, Meylan, France, 1998.
[12] Drylab, Molnar Institute für angewandte Chromatographie, Berlin, Germany, 2000.
[13] J.W. Dolan, D.C. Lommen, L.R. Snyder, J. Chromatogr. 485 (1989) 91.
[14] A. Vasanits, D. Kutlán, P. Sass, I. Molnár-Perl, J. Chromatogr. A 870 (2000) 271.
[15] D. Kutlán, I. Molnár-Perl, J. Chromatogr. A 987 (2003) 311.
[16] E.A. Hogendoorn, E. Dijkman, S.M. Gort, R. Hoogerbrugge, P. van Zoonen, U.A.T. Brinkman, J. Chromatogr. Sci. 31 (1993) 433.
[17] S.M. Gort, E.A. Hogendoorn, E. Dijkman, P. van Zoonen, R. Hoogerbrugge, Chromatographia 42 (1996) 17.
[18] Ch.H. Lee, J.W. Lee, K.H. Row, J. Chromatogr. A 828 (1998) 337.
[19] G. Vivó-Truyols, J.R. Torres-Lapasió, M.C. García-Alvarez-Coque, J. Chromatogr. A 1018 (2003) 169.
[20] G. Vivó-Truyols, J.R. Torres-Lapasió, M.C. García-Alvarez-Coque, J. Chromatogr. A 1018 (2003) 183.
[21] J.R. Torres-Lapasió, J.J. Baeza-Baeza, M.C. García-Alvarez-Coque, Anal. Chem. 69 (1997) 3822.
[22] J.P. Foley, J.G. Dorsey, Anal. Chem. 55 (1983) 730.
[23] P. Jandera, J. Chromatogr. 485 (1989) 113.
[24] S. Carda-Broch, J.R. Torres-Lapasió, M.C. García-Alvarez-Coque, Anal. Chim. Acta 396 (1999) 61.
[25] S.J. López-Grío, G. Vivó-Truyols, J.R. Torres-Lapasió, M.C. García-Alvarez-Coque, Anal. Chim. Acta 433 (2001) 187.
[26] G. Vivó-Truyols, J.R. Torres-Lapasió, M.C. García-Alvarez-Coque, Chromatographia 56 (2002) 699.
[27] V. Concha-Herrera, G. Vivó-Truyols, J.R. Torres-Lapasió, M.C. García-Alvarez-Coque, Anal. Chim. Acta 518 (1994) 191.
[28] J.D. Stuart, D.D. Lisi, L.R. Snyder, J. Chromatogr. 485 (1989) 657.
[29] J.W. Dolan, L.R. Snyder, N.M. Djordjevic, D.W. Hill, T.J. Waeghe, J. Chromatogr. A 857 (1999) 21.